

Published in final edited form as:

Int J Biol Macromol. 2014 February ; 63: 64–74. doi:10.1016/j.ijbiomac.2013.10.029.

Human cytidine deaminase: A biochemical characterization of its naturally occurring variants

Daniela Micozzi^a, Francesco Martino Carpi^a, Stefania Pucciarelli^a, Valeria Polzonetti^a, Paolo Polidori^b, Santiago Vilar^d, Brian Williams^e, Stefano Costanzi^{e, **}, and Silvia Vincenzetti^{c, *}

^aSchool of Biosciences and Biotechnology, University of Camerino, via Gentile III da Varano, 62032 Camerino, MC, Italy

^bSchool of Pharmacy, University of Camerino, via circonvallazione 93/95, 62024 Matelica, MC, Italy

^cSchool of Veterinary Medical Sciences, University of Camerino, via circonvallazione 93/95, 62024 Matelica, MC, Italy

^dDepartment of Organic Chemistry, Faculty of Pharmacy, University of Santiago de Compostela, Santiago de Compostela 15782, Spain

^eDepartment of Chemistry, American University, Washington, DC 20016, USA

Abstract

Human cytidine deaminase is an enzyme of the pyrimidine salvage pathways that metabolizes several cytosine nucleoside analogs used as prodrugs in chemotherapy. We carried out a characterization of the cytidine deaminase 79A>C and 208G>A Single Nucleotide Polymorphisms, in order to highlight their functional role and provide data that could help fine-tune the chemotherapeutic use of cytosine nucleosides in patients carrying the above mentioned SNPs. The 79A>C SNP results in a K27Q change in a protein region not involved in the catalytic event. The 208G>A SNP produces an alanine to threonine substitution (A70T) within the conserved catalytic domain. Q27 variant is endowed with a greater catalytic efficiency toward the natural substrates and the antileukemic agent cytarabine (Ara-C), when compared to K27 variant. Molecular modeling, protein stability experiments and site-directed mutagenesis suggest that K27 variant may have an increased stability with respect to Q27 due to an ionic interaction between a lysine residue at position 27 and a glutamate residue at position 24. The T70 variant has a lower catalytic efficiency toward the analyzed substrates when compared to the A70 variant, suggesting that patients carrying the 208G>A SNP may have a greater exposure to cytosine based pro drugs, with possible toxicity consequences.

Keywords

Cytidine deaminase; Genetic polymorphism; Kinetic analysis; Molecular modeling; Site-directed mutagenesis

1. Introduction

Cytidine deaminase (CDA, cytidine/2'-deoxycytidine aminohydrolase; EC 3.5.4.5, gene map locus 1p36.2-p35) is an enzyme of the pyrimidine salvage pathways, which catalyzes the formation of uridine and 2'-deoxyuridine by hydrolytic deamination of cytidine and 2'-deoxycytidine, respectively. Human CDA is a tetrameric enzyme of identical 15 kDa subunits, each containing an essential zinc atom in the active site, which is coordinated by three negatively charged cysteines (C65, C99, C102) and a glutamic acid residue located in position 67. The zinc atom plays an important role in the catalytic process. The particularity of this enzyme is that the active site of one monomer is constructed by amino acid residues coming from the other three subunits through a complicated set of inter-subunit interactions. Despite this, cooperation between subunits and substrate binding was not observed in the tetrameric CDA [1–3].

The expression of CDA mRNA was observed at high levels in liver and placenta and low levels in lung and kidneys, while no expression was detected in heart, brain and muscle [4]. High CDA activity was reported in liver and spleen and moderate activity was found in lung, kidney, large intestinal mucosa and colon mucosa [5]. No appreciable amount of this enzyme was found in skeletal muscle, bone, or cartilage. High concentration of CDA was found in mature neutrophils, with levels many times greater than in other blood elements such as lymphocytes. CDA is also a marker for myeloid cell differentiation, since the expression level of its mRNA increases with their maturation [6,7]. Furthermore, CDA was identified as a growth inhibitor of granulocyte-macrophage colony-forming cells [8,9]. CDA levels are elevated in serum and synovial fluid in rheumatoid arthritis, reflecting an increase in neutrophil breakdown in the synovial fluid during joint inflammation and remains independent of age, sex, and disease duration [10].

The clinical interest around human CDA is due to its ability to deaminate both its natural substrate as well as several chemotherapeutic agents, such as the anti-leukemic agent Ara-C, the anti-cancer agents 5'-azadeoxycytidine (Aza-CdR) and 2',2'-difluorodeoxycytidine (gemcitabine, dFdC). The deamination of these agents leads to their pharmacological inactivation. For this reason, the CDA inhibitor tetrahydrouridine (THU) is often co-administered with cytidine analogs in order to improve their pharmacokinetics and pharmacodynamics [11].

It is well known that CDA is an enzyme that tends to polymorphism: in human granulocytes Teng and coworkers [12] observed the presence of three electrophoretic CDA phenotypes and proposed that they are the homozygous and heterozygous expressions of two alleles. Subsequently, two different research groups identified two cDNA sequences coding for two CDA variants that revealed one non-conservative amino acid substitution at position 27 of the amino acidic sequence. CDA1 was found to carry a glutamine (Q) residue [6] and CDA2 was found to carry a lysine (K) residue at this position [4]. Other research groups have identified these findings as well [13,14]. It was later identified that one SNP in the CDA gene, 79A>C, results in a K27Q change inside the coding region. This polymorphism was present in the DNA of both African and Caucasian American subjects with allele frequencies of 10.8% and 29.8%, in African American and Caucasian American subjects, respectively [15]. A study on K27Q genotype frequency in Italian population was 0.328, 0.469 and 0.203 for K*/K*, K*/Q*, and Q*/Q*, respectively. The frequency of the Q*/Q* genotype was higher in Italians compared to all other populations [16]. Some authors have reported a moderate decrease in the level of CDA activity in the K27Q polymorphism, which was associated with a modest alteration in the apparent K_m value [14,15]. A study conducted on 221 Japanese subjects, reported an allele frequency of 21% for 79A>C without a change in enzymatic activity between the mutant and the wild-type CDA after expression

in yeast in presence of cytidine or 1- β -D-arabino furanosylcytosine (cytarabine, Ara-C) [17]. In the Chinese population, the incidence of CDA 79A>C SNP was 12.0% and 12.3% in cancer patients and in healthy volunteers, respectively. Furthermore Chinese patients carrying 79A>C variant were observed to be more prone to developing severe neutropenia after gemcitabine-based chemotherapy [18]. The substitution at position 27 of the amino acid sequence lies in a protein region close to a highly conserved region in most of the tetrameric CDAs but seems not to be directly involved in the catalytic process. The *pI* values observed for the two variants Q27 and K27 were, *pI* = 4.50 and *pI* = 5.0 respectively [19].

Other authors investigated the role of another SNP in the human CDA gene, 208G>A, that produces an alanine to threonine substitution (A70 T) within the conserved catalytic domain (₆₅CAERTA₇₀). The SNP 208G>A was not detected in Europeans, whereas the allelic frequency of 208A was 0.125 in Africans [20]. According to the two previous studies [17,20], frequencies of homozygous 208G>A individuals in the Japanese and African populations were estimated to be about 0.18% and 1.56%, respectively. Finally, in a recent study the 208G>A polymorphism appears to be very rare in the adult Indian population [21], whereas in the Chinese population the frequency for 208G>A polymorphism was found to be of 1.0%, and no Chinese cancer patients were found to be homozygous or heterozygous for this variant allele [18].

Inter-individual variation in the activity of cytidine deaminase due to the abovementioned polymorphisms can substantially affect the concentration of prodrug present in the blood, which influences both the efficacy and safety of the chemotherapeutic treatment [17,22]. For example, functional studies demonstrated that A70T CDA showed a 40% activity for cytidine and 32% for Ara-C as substrates, with respect to the K27 CDA [17]. Therefore, a population characterized with 208A genotype may be more sensitive to Ara-C treatment than its prototype. Other authors reported the case of a cancer patient treated with gemcitabine plus cisplatin that was found to be homozygous for the SNP 208G>A in exon 2 of the CDA gene. This SNP produced an A70 T variant of CDA and showed a decrease in deaminase activity and an increase in plasma gemcitabine levels which led to severe drug toxicity [23,24]. Moreover, it has been demonstrated that patients with reduced CDA activity may suffer from severe adverse drug reactions [25,26] upon the treatment with dFdC, a chemotherapeutic agent used against various solid tumors, such as breast cancer, pancreatic cancer and non-small cell lung cancer. This drug is largely metabolized by CDA to produce the inactivated metabolite, dFdU [27]. On the other hand, patients with excessive CDA activity may require the administration of higher doses of prodrug or CDA inhibitors.

From these observations, it is evident that the analysis of the CDA polymorphism can help to establish gene-based information for the treatment of cancer [28–32]. In particular, such pharmacogenetic studies can help predict the efficacy and toxicity of cytidine-based drugs based on the genetic profile of the patient. Thus, in this work we characterized the kinetics and biochemical properties of the most common variant, as well as variants that arise from the naturally occurring SNPs 79A>C and 208G>A. For clarity, in this work we named the most common variant K27/A70, the variant arising from the 79A>C polymorphism Q27/A70, and the variant arising from the 208G>A polymorphism K27/T70. Moreover, in order to generate hypotheses on the structural differences between the K27/A70 and Q27/A70 variants we carried out a molecular modeling study comparing the crystal structures of human (1MQ0) and murine (2FR5) CDA [33,34], in which the residue at position 27 is a Q or a K, respectively. Finally, to substantiate the model-derived hypothesis that the lysine residue at position 27 establishes an ionic bond with glutamate at position 24, a mutant CDA E24Q was generated using the K27/A70 variant as a template. The substitution of the glutamate with a glutamine residue was chosen to prevent the ionic interaction between the carboxyl group of glutamate and the amino epsilon group of lysine, while at the same time

maintaining similar steric features. The novelty of the present work consists in a deep kinetic characterization of the three variants especially concerning the inhibition studies that were made through a set of inhibitors that may be used to selectively reduce the deaminase activity of the K27/A70 or the Q27/A70 variant.

2. Materials and methods

2.1. Compounds

Dithiothreitol (DTT) and isopropyl-thio- β -D-galactopyranoside (IPTG) were purchased from ICN Biochemicals (Aurora, OH), ampicillin from USB (Cleveland, OH). Cytidine (CR), deoxycytidine (CdR), Tris (hydroxymethyl) aminomethane (trizma base) and other reagents were obtained from Sigma Chemical Co. (St. Louis, MO). PM10 membranes were purchased from Amicon Corporation (Beverly, MA); DEAE 52 was produced by Whatman (UK), whereas Superdex 75 HR 10/30, MonoQ HR5/5 and the HPLC system Äkta Purifier were purchased from GE Healthcare (Uppsala, Sweden). “Quikchange Site-Directed Mutagenesis” kit was purchased from Stratagene (Stratagene, La Jolla, CA). Plasmid DNA was isolated using the Qiagen plasmid midi kit (Qiagen, Milan, Italy) or by NucleoSpin plasmid (Macherey-Nagel, M. Medical, Milan, Italy). Primer synthesis was done by Sigma Chemical Co. (St. Louis, MO) whereas DNA sequences were done by BMR Genomics (Padova, Italy). Restriction nucleases were obtained from Promega (Madison, WI). Mini protean III electrophoresis apparatus and Low range protein markers were purchased from Bio-Rad (Hercules, CA).

2.2. DNA techniques

The pyrimidine requiring CDA-negative derivative of MC1061, *Escherichia coli* SØ5201 (MC1061 cdd:pyrD:Kan) was used as host. The mutations A70T (generating the variant K27/T70) and E24Q were introduced by site-directed mutagenesis using the “QuikChange Site-Directed Mutagenesis Kit” (Stratagene, La Jolla, CA) that allows site-specific mutations in a double-stranded plasmid. The plasmid pTrcHUMCDA2 (K27/A70) was used as a template, containing the human CDA cDNA on a 446 bp NcoI-BamHI fragment in pTrc 99-A [35]. The primers (Table 1), each complementary to the opposite strand of the vectors were extended by PCR reaction. The PCR product was treated with restriction endonuclease *DpnI* to digest the parental template. Each resulting plasmid DNA, pTrcHUMA70T and pTrcHUME24Q, was subsequently transformed into competent cells of *E. coli* SØ5201. DNA sequence analysis confirmed the correct position of the mutation.

2.3. Enzymes preparation

To further clarify the role of residue 27 in enzyme functionality and its interaction with residue E24, the mutant E24Q CDA was generated and the expressed protein was purified and characterized.

Site-directed mutagenesis was carried out to obtain the pTrcHUMA70T and pTrcHUME24Q plasmids that were transformed into the pyrimidine requiring *E. coli* strain SØ5201, in order to express the mutant protein A70T (K27/T70) and E24Q.

At this purpose, *E. coli* SØ5201 (MC1061 cdd:pyrD:Kan) containing the plasmid pTrcHUMCDA1 [35] or pTrcHUMCDA2 [19] were used as a source of cytidine deaminase Q27/A70 and K27/A70 respectively. The purification of the K27/A70, Q27/A70, and K27/T70 variants, was performed as described previously [1]. Briefly, cultures of *E. coli* SØ5201 (500 mL), harboring pTrcHUMCDA1 (Q27/A70), pTrcHUMCDA2 (K27/A70), pTrcHUMA70T (K27/T70) and pTrcHUME24Q (E24Q) were grown at 37 °C in L-broth and supplemented with 100 μ g/mL ampicillin. The protein expression was induced during

late exponential growth ($A_{436\text{ nm}} = 1.0$) by the addition of 1 mM IPTG. After 19 h of shaking at 37 °C, the cells were harvested by centrifugation at 5000xg, washed with 0.9% NaCl and re-suspended in buffer A (Tris-HCl 50 mM, pH 7.5, 1 mM DTT, 1 mM EDTA). After sonic disruption, each crude extract was loaded onto a DEAE-52 anionic exchange chromatography, equilibrated with buffer A, and eluted by a linear gradient between buffer A and buffer B (buffer A + 0.5 M KCl). The fractions containing the enzyme were pooled, concentrated by ultrafiltration on a PM 10 membrane, and loaded onto a gel for filtration on Superdex 75 HR 10/30 connected to an HPLC system (Äkta Purifier), equilibrated with buffer A. The elution of the column was achieved in the same buffer. The CDA fractions eluted from gel filtration were concentrated by ultrafiltration and finally loaded onto a Mono Q HR5/5, performed in HPLC. The column was equilibrated in buffer A and eluted by a step gradient between buffer A and buffer B. After the last purification step each CDA functional variant and mutant enzyme, were dialyzed by ultrafiltration on a PM 10 membrane against buffer A.

Protein concentration was determined by the Bradford protein assay [36]. Sodium dodecyl sulphate polyacrylamide gel electrophoresis (SDS-PAGE) was performed as described by Laemmli [37], using 15% acrylamide and the Mini Protean II apparatus (Bio-Rad, gel size 7 cm × 8 cm × 0.75 mm). The markers used were Bio-Rad low range.

2.4. Kinetic experiments, effect of temperature on enzymes activity

CDA activity assays and kinetic studies on the functional variants Q27/A70, K27/A70, K27/T70 as well as of the mutant enzyme E24Q, were performed as previously described [35], in presence of several substrates and inhibitors of cytidine deaminase.

One enzyme unit is defined as the amount of enzyme which catalyzes the deamination of 1 μ mole of cytidine per minute at 37 °C. The effect of temperature on the enzymatic activity of the functional variants and mutant CDA was investigated at temperatures ranging from 5 to 75 °C. The temperature dependence of V_{max} and K_{m} values of recombinant CDAs was also analyzed by using the empirical Arrhenius equation ($\ln V_{\text{max}} = \ln A - E_{\text{a}}/RT$) and the van't Hoff equation ($\ln K_{\text{m}} = -\Delta H/RT + \Delta S/R$).

In these experiments the experimental error in the measurements of the enzymatic activity has been determined by performing repeated assays every 30 min during 8 h time span. The relative error in the measurement of the initial velocity resulted to be 6% of the observed value.

2.5. Oxidative resistance experiments

The enzymatic stability of each CDA variant was investigated in presence of sodium hypochlorite, NaOCl (0–1400 μ M) and hydrogen peroxide, H_2O_2 (0–50 mM), as oxidizing agents [38]. The stock concentration of the oxidants was estimated by measuring the absorbance at 230 nm (H_2O_2) and 290 nm (NaOCl), using absorption coefficients of 72.4 and 317 $\text{M}^{-1}\text{ cm}^{-1}$ for H_2O_2 and NaOCl, respectively. In this experiment, 2.6 μ g of each CDA variant or mutant protein were separately incubated at 37 °C with different NaOCl or H_2O_2 concentrations, in a final volume of 50 μ l, at incubation times of 5, 15, 15, 35, 45, 60 min. After each incubation period, CDA activity was observed as described above.

2.6. Molecular modeling

All the molecular modeling procedures were performed with the Schrodinger molecular modeling suite [39] and were based on the crystal structure of murine (2FR5) and human (2MQ0) cytidine deaminase [33,34]. In particular, the 2FR5 structure was studied as an example of a K27/A70 variant, while the 2MQ0 was studied as a variant of the Q27/A70

variant. Another structure was obtained by modifying the K27 residue in the 2FR5 structure, in which the lysine at position 27 of the K27/A70 variant was substituted with its chloramine derivative.

The crystal structures were subjected to the “protein preparation wizard” workflow to add hydrogen atoms, calculate the protonation states of all ionizable groups at pH 7, and optimize the orientation of hydroxyl groups, Asn, Gln and His residues. The workflow ended with a constrained energy minimization of the hydrogen atoms that allowed maximum root mean square deviations (RMSD) of 0.30 Å.

Following the “protein preparation wizard” workflow, the structures were subjected to a Monte Carlo conformational search with the MacroModel (MacroModel, version 9.9) molecular mechanics engine implemented in the Schrodinger suite. In these calculations, full flexibility was granted to the residues at residues 24 and 27, as well as all residues with at least one atom within a radius of 5 Å from the former. An additional shell of residues located within 3 Å of the flexible atoms were included in the calculation of the potential energy of the system, but were held rigid. The conformational searches were based on 1000 steps of the Monte Carlo Multiple Minimum algorithm conducted with the OPLS 2005 force field and the cutoff value on the energy gradient for the energy minimizations was set to 0.05 kJ/(mol Å). For each conformational search, the lowest energy structures, as well as all the structures within 20 kJ/mol from the former, were saved in the output file and analyzed.

3. Results

3.1. Expression and purification of mutant proteins

Through this work we carried out kinetic and molecular studies on the functional variants Q27/A70, K27/A70 and K27/T70, in order to gather data that could be helpful in the design of more efficient cytidine-based chemotherapeutic drugs, which can be administered to patients carrying the 79A>C and 208G>A SNPs.

The three variants K27/A70, Q27/A70 and K27/T70, as well as the mutant E24Q, were purified as described previously in the Materials and Methods section and the final enzyme preparations were judged >95% pure after 15% SDS-PAGE (Fig. 1). DNA sequence analysis performed on each mutant cDNA confirmed the correct position of each mutation. For clarity, the residues present in each CDA variant/mutant are displayed in Table 2.

3.2. Kinetic experiments

Table 3 shows the K_m and V_{max} values for the functional variants K27/A70, Q27/A70, K27/T70 and for the active mutant E24Q, regarding the naturally occurring substrates such as CR, CdR, and cytosine nucleoside analogs, which are used in chemotherapy as antitumor agents. The results indicated that the variant Q27/A70 has a moderately increased catalytic efficiency toward the natural substrates and toward the antileukemic agent Ara-C with respect to the K27/A70 variant. However, the trend is the opposite for the substrates Aza-CdR, 6-aza-CR, and fazarabine, which are deaminated somewhat more efficiently by the K27/A70 variant.

The K27/T70 variant showed a very low catalytic efficiency (about 100 fold lower than those of functional variants) for all substrates. As shown in Table 3 this low catalytic efficiency is due to a decreased catalytic rate, since the substrate affinity is substantially similar to that of Q27/A70 and K27/A70 variants. The mutant E24Q showed a decreased catalytic efficiency for the assayed substrates due to decreased substrate affinity, whereas the catalytic rate was similar to that of the functional Q27/A70 variant. Interestingly, the V_{max} value for the mutant E24Q with substrate, Aza-CdR, was found to be substantially less

than the two natural substrates and Ara-C. The compound 2',3'-CdR is not substrate of the CDA functional variants or the E24Q mutant enzyme.

The ability of a number of nucleosides and nucleotides to inhibit the three above mentioned variants and the mutant E24Q was tested. The resulting K_i values (Table 4) indicated, a significantly higher affinity of THU and 5-F-zebularine for the Q27/A70 variant with respect to K27/A70 and K27/T70 variants. Conversely pseudoisocytidine, was more efficient on the K27/A70 variant. Finally, for all the inhibitors tested, the E24Q mutant showed slightly increased K_i values with respect to the three CDA functional variants.

3.3. Effect of temperature on enzyme activity

The effect of temperature on enzyme activity and stability of the three variants and of the E24Q mutant was also investigated, as described under Materials and Methods. The optimal temperature for the enzymes was obtained by plotting the percentage of V_{\max} as a function of increasing temperatures. The two variants Q27/A70 and K27/A70 are particularly active at high temperatures; from 10 to 50 °C the V_{\max} % of K27/A70 variant was slightly higher with respect to Q27/A70 variant. These two variants reached 100% V_{\max} at 60 °C for Q27/A70 and 65 °C for K27/A70. However, when the temperature was raised to 72 °C, the Q27/A70 variant exhibited a greater thermo-stability with respect to the K27/A70 variant (Fig. 2). Above this temperature the V_{\max} (%) of the two enzymes slowly decreased even if they showed a V_{\max} of about 60% at 80 °C.

The functional variant K27/T70 also showed a high enzymatic activity at low temperatures with an optimal temperature around 30 °C. Above this temperature the K27/T70 variant showed a slow decrease in activity, with a 65% V_{\max} value that was stable until 80 °C.

The behavior of the E24Q mutant as temperature increased was very different with respect to the K27/A70 and Q27/A70 variants. The enzymatic activity increased significantly at temperatures above 50 °C with an optimal temperature of 65 °C. Above this temperature the activity decreased immediately (Fig. 2).

The temperature dependence of V_{\max} and K_m values of K27/A70, Q27/A70, K27/T70 and E24Q was also analyzed by Arrhenius and van't Hoff equations. The energy of activation (E_a) value calculated for the Q27/A70 variant was 9.304 kcal/mol, which was very close to that observed in the K27/A70 variant (9.038 kcal/mol, see also [3]). Through the van't Hoff plot a discontinuity in the temperature dependence of K_m for K27/A70 was observed, in which the enthalpy values for the interaction between substrate and the enzyme were calculated to be $\Delta H = 3.57$ kcal/mol for temperatures between 10 and 35 °C, and $\Delta H = -8.88$ kcal/mol between 35 and 80 °C (Fig. 3A). Conversely, this discontinuity was not observed in the van't Hoff plot for the Q27/A70 variant and the enthalpy of the interaction between substrate and enzyme was $\Delta H = -8.149$ kcal/mol (Fig. 3B).

A discontinuity in van't Hoff linearization is observed for the K27/T70 variant centered at approximately 35 °C. In this case the energetics of substrate binding is still enthalpically favorable at low temperatures. In fact, the enthalpy values for the interaction between substrate and enzyme, were $\Delta H = -14.72$ kcal/mol at temperatures 10–35 °C and $\Delta H = -1.88$ kcal/mol at temperatures 40–80 °C (Fig. 3C). The presence of a threonine residue in position 70 appears to markedly reduce the interactions between substrate and active site residues at high temperatures.

In the case of the E24Q mutant no discontinuity was observed in the van't Hoff plot (Fig. 3D) and the thermodynamic behavior displayed for the formation of the enzyme/substrate complex was very similar to that of the Q27/A70 variant.

The Eyring plot allowed for the calculation of the entropy and enthalpy of activation. The values of enthalpy and entropy of activation for the K27/A70 and Q27/A70 variants were found to be very similar, $\Delta H = 8.408$ kcal/mol and 8.662 kcal/mol and $\Delta S = -22.992$ cal/mol and -23.52 cal/mol respectively (Fig. 4A and B).

The K27/T70 variant exhibits a very uncommon Eyring plot (Fig. 4C), with a very steep slope at low temperatures and an almost flat trend at high temperatures. By analyzing the linear region of this plot, between 10 and 35 °C, we obtained an enthalpy and entropy of activation of, $\Delta H = 15.96$ kcal/mol and $\Delta S = 0.584$ cal/mol. At higher temperatures the enzyme seems to exert its catalytic function without any dependence on temperature, as if it were only under the control of entropy; for this reason we did not fit these parts of the data by using the Eyring equation. The unusual flatness of the k_{cat} temperature dependence of the K27/T70 variant remains unexplained; we might suggest that the more intense fluctuations as temperature is increased to above 35 °C interfere with substrate binding as shown by the strong reduction of enthalpy of binding from van't Hoff analysis (Fig. 4C). Apparently the introduction of a threonine residue rather than alanine in the very conserved $_{65}\text{CAERTA}_{70}$ motif has a strong effect on the energy of the transition state, likely by modifying the flexibility of the active site, which on the other hand becomes more resistance to thermal inactivation.

For the E24Q mutant (Fig. 4D) the enthalpy of activation was calculated as $\Delta H = 14.351$ kcal/mol and the entropy of activation as $\Delta S = -4.95$ cal/mol.

3.4. Oxidative resistance experiments

The oxidative resistance experiments for the Q27/A70, K27/A70, K27/T70 variants and the E24Q mutant were performed as described in Section 2, using two oxidizing agents with different oxidative potential; sodium hypochlorite and hydrogen peroxide.

The resistance to increasing concentration of each oxidizing agent was evaluated by plotting the percentage of CDA activity as a function of time of exposure to the oxidizing agent.

Inhibition of K27/A70, Q27/A70 and K27/T70 by 100 μM NaOCl occurred in a time-dependent manner and after 60 min of incubation the residual activity reached the value of 32% for K27/A70, 49% for Q27/A70 and 27.5% for K27/T70 (Fig. 5A). The concentration of NaOCl at 50% inhibition of activity of the variants ($K_{0.5}$ value) was observed to be 100 μM and 60 μM , for the Q27/A70 and K27/A70 variants respectively, with the K27/T70 variant showing similar behavior to that of K27/A70 (Fig. 5B).

When H_2O_2 was used as oxidizing agent (Fig. 5C) the oxidation resistance of the two variants K27/A70 and Q27/A70 was reversed. In fact, the $K_{0.5}$ values for H_2O_2 were 15.0 and 23.5 mM for Q27/A70 and K27/A70 respectively (Fig. 5D). The K27/T70 variant was more sensitive to the oxidizing agent H_2O_2 , with respect to K27/A70 and Q27/A70 variants, with a $K_{0.5}$ value of 11.5 mM.

The E24Q mutant was surprisingly resistant to the oxidative activity of NaOCl, with a 97% residual activity after 60 min of incubation, with the highest $K_{0.5}$ of 1 mM (Fig. 6A and B). In the presence of H_2O_2 , the E24Q mutant showed a $K_{0.5}$ of 8.0 mM (Fig. 6C and D).

3.5. Molecular modeling

Molecular modeling studies were conducted in order to generate hypotheses on the structural differences between the K27/A70 and Q27/A70 variants. In particular, the murine 2FR5 structure was studied as an example of the K27/A70 variant, while the human 2MQ0 structure was studied as an example of the Q27/A70 variant [33,34]. Moreover, in light of

the fact that the K27/A70 variant is less resistant than the Q27/A70 to oxidation with NaOCl, a further structure of the K27/A70 variant, in which the lysine at position 27 was substituted with its chloramine derivative, was obtained by modifying the K27 residue in the 2FR5 structure. These three structures were subjected to 1000 steps of Monte Carlo conformational search with the MacroModel engine of the Schrodinger suite (MacroModel, version 9.99, see also [39]). The results of the conformational searches suggest that, in the K27/A70 variant, an ionic interaction keeps the side chain of K27 closely associated with the side chain of E24, which is located upstream in the same α -helix, with an average distance between the nitrogen atom of the side chain of K27 and the carboxyl carbon atom of E24 of 3.25 ± 0.07 Å. The models also suggest that the distance between the side chains of residues 27 and 24 changes dramatically if the ionic interaction between the two residues is disrupted by the exchange of the lysine with a glutamine residue or the conversion of the lysine to its chloramine derivative. Specifically, for the models of the Q27/A70 variant and the K27/A70 variant in which K27 was modified to its chloramine derivative, we detected substantial increases in the distance between the residues at position 27 and 24, with an average distance between the nitrogen atom of the side chain of Q27 or K27 and the carboxyl carbon atom of E24 of 6.72 ± 1.12 Å and 4.74 ± 1.14 Å, respectively. Fig. 7 shows a plot of the distances between the nitrogen atom of the side chain of Q27 or K27 and the carboxyl carbon atom of E24 for all the conformations generated through our Monte Carlo conformational searches, ranked in order of relative potential energy with respect to the most stable structure. Moreover, Fig. 8 shows a molecular representation of the relationship between the two residues at position 27 and 24 in the 10 lowest energy structures resulting from the conformational search for the K27/A70 variant, the Q27/A70 variant, and the K27/A70 variant in which K27 was modified to the corresponding chloramine derivative.

4. Discussion

The effectiveness of a drug treatment can be affected by inter-individual variations of the drug targets, as well as the enzymes that metabolize both drugs and prodrugs. Therefore the analysis of drug targets and enzymes for polymorphism provides useful information for the development of personalized treatments. Specifically in relation to CDA, such analyses could be used for the optimization of treatments of cancer patients. Recently several research groups carried out studies on single-nucleotide polymorphisms in the human cytidine deaminase gene [15,17,24], as already discussed in the introduction section. In particular, Baker and co-workers [40] performed a functional analysis of genetic variants of cytidine deaminase and deoxycytidine kinase. The authors used purified recombinant enzymes resulting from the non-synonymous SNPs of CDA to evaluate their impact on gemcitabine (dFdC), an anticancer prodrug not assayed in our study. The authors found that the K27Q and A70T substitutions do not affect the CDA activity toward dFdC. Moreover, they demonstrated that the A70T, but not K27Q substitution, affects the CDA activity toward the antileukemic agent Ara-C.

In this work kinetic and molecular studies on the CDA variants K27/A70, Q27/A70 and K27/T70 were performed, in order to understand their functional role and also to design cytidine based drugs to be administered to patients carrying the 79A>C and 208G>A SNPs.

Beyond confirming and corroborating the properties of the CDA functional variants reported in the literature [14,16,24,40], we subjected the three functional variants to an in depth kinetic characterization, concentrating on a set of inhibitors that could be used to selectively reduce the deaminase activity of the K27/A70 or the Q27/A70 variant.

A visual inspection of the crystal structure of the Q27/A70 variant of the human CDA (2MQ0) shows that the residue at position 70 is relatively close to the catalytic site, while

the residue at position 27 is located further away (Fig. 9). Specifically, the co-crystallized diazepinineriboside is found at a distance of 9.6 Å from the α -carbon of the residue at position 70 and 12.3 Å from the α -carbon of the residue at position 27. Moreover, residue 70 is located in the middle of an α -helix that originates from the catalytic site and harbors three crucial residues. C65 which is one of the three cysteine residues that coordinate the catalytically essential Zn^{2+} ion, A66, which establishes hydrogen bonds with the ligand through its backbone, and E67, which establishes hydrogen bonds with the ligand through its side chain and is fundamental for the catalytic mechanism. On the other hand, residue 27 is located on a different α -helix that is separated from the binding site by an antiparallel β -sheet.

As shown in Table 3, the Q27/A70 and K27/A70 variants showed slight differences in the rate of deamination of the physiological substrates cytidine and deoxycytidine. Conversely, the K27/A70 variant showed a ten-fold decrease in catalytic efficiency (V_{max}/K_m) toward Ara-C with respect to the Q27/A70 variant. This significant change of the catalytic efficiency is due to a lower catalytic rate and also an impaired substrate recognition. These data suggest that patients carrying the 79A>C (Q27/A70) polymorphism may inactivate cytarabine more efficiently than those with the more common K27/A70 variant, which would render this prodrug pharmacologically inactive. This could mean that patients with the Q27/A70 variant should be treated with higher doses of the pro-drug to achieve the same pharmacological effect of the patients carrying K27/A70 variant. However, the differences on the Ara-C deamination rate between Q27/A70 and K27/A70 variants found in our work differ from the data of Baker and coworkers who found no significant differences in the Ara-C deamination between these two variants [40].

No substantial differences were found in the rate of deamination for the three functional variants (K27/A70, Q27/A70 and K27/T70) toward the compounds Aza-CdR, 6-aza-CR. However, a 3-fold increase in catalytic efficiency toward fazarabine was found for the K27/A70 variant with respect to the Q27/A70 and K27/T70 variants.

The Q27/A70 variant is more susceptible to the action of tetrahydrouridine and 5-F-zebularine than the K27/A70 variant (Table 3), suggesting that patients harboring the product of 79A>C can be treated more efficiently with these two CDA inhibitors in order to increase the effectiveness cytidine analog drugs [41]. Conversely the K27/A70 variant was observed to be more susceptible to the effect of pseudoisocytidine than the other variants. This result may indicate that it is possible to perform a customized and targeted therapy for a patient by choosing the inhibitor that results in the greatest efficient for that the particular polymorphism.

As the crystal structures reveal, residue 27 is rather far from the catalytic site (Fig. 8). For instance, in the murine CDA structure solved in complex with THU (2FR5), the distance between the closest atoms of K27 and the bound THU molecule is 11.4 Å. Hence, the different kinetic properties of the K27/A70 and Q27/A70 variants most likely arise from the global effect of the substitution on the tertiary structure of the protein. Similar long-distance effects of mutations, which in some cases are very pronounced, have been detected for a wealth of enzymes and proteins in general [42–45].

The K27/T70 variant showed a very low catalytic efficiency (about 100 fold) with respect to the other two functional variants. Since the K_m value for the substrates cytidine, deoxycytidine and Ara-C remained unchanged, this decrease in catalytic efficiency is due its low catalytic rate with respect to Q27/A70 and K27/A70. This is also confirmed by the fact that K27/T70 variant showed K_i values toward CDA inhibitors that were very similar to those found in the two other functional variants (see also Table 4). These results are in

agreement with those obtained by Sugiyama and coworkers [24], who found that this K27/T70 variant considerably loses its deamination activity toward gemcitabine, and also confirmed that patients carrying the 208G>A SNP may show severe adverse reactions due to increased plasma levels of the chemotherapeutic agent.

The effect of temperature on the enzymatic activity of Q27/A70, K27/A70, and K27/T70 variants was evaluated. The two variants K27/A70 and Q27/A70, proved to be thermostable in presence of increasing temperatures. The behavior of K27/T70 was observed to be different from the other two functional variants, with increased enzymatic activity at low temperatures with an optimal activity around at 30 °C. Above this temperature the K27/T70 variant is stable (mean V_{\max} % = 65) until 80 °C.

The van't Hoff plot for the K27/A70 variant (Fig. 3A) showed two different temperature ranges corresponding to different binding energies for the substrate [3]. In the temperature range of 10–35 °C the enthalpy of binding is endothermic ($\Delta H = 3.57$ kcal/mol), whereas in the temperature range of 35–80 °C it is exothermic ($\Delta H = -8.88$ kcal/mol). This may indicate that a conformational modification may occur in the temperature range around 35 °C, which leads to a stronger interaction with the substrate deoxycytidine [3]. On the contrary, the van't Hoff plot of the Q27/A70 variant showed an exothermic value of $\Delta H = -8.1495$ kcal/mol, very close to that observed for the K27/A70 variant, in the temperature range of 37–80 °C, which indicates that the interaction with the substrate deoxycytidine is enthalpically favorable at all temperatures considered for the Q27/A70 variant (Fig. 3B).

However, the Arrhenius (data not shown) and Eyring plots (Fig. 4A and B), show that the energy of activation (E_a) and the enthalpy activation values for Q27/A70 and K27/A70 variants are very close. This means that these two variants are able to reach the transition state in the same manner. Furthermore, considering the value of the entropy of activation for the two variants, the geometry of the enzymatic reaction seems unaffected by the aminoacidic substitution.

The presence of a threonine residue in position 70 had a pronounced effect on the energy of the interaction between substrate and the enzyme's active site, in the presence of high temperatures as evidenced by the van't Hoff (Fig. 3C). On the other hand in the same temperature range the activation enthalpy was near zero (Fig. 4C). These results could reflect the low catalytic efficiency (V_{\max}/K_m) shown by this variant with respect to all of the substrates assayed (see Table 3).

The stability of the four CDAs was also evaluated by a study based on their resistance to the oxidizing agents. Two oxidizing agents, sodium hypochlorite and hydrogen peroxide, were used each with a different oxidative potential. The behavior of the K27/A70 and Q27/A70 variants depended on the type of oxidizing agent used. In presence of NaOCl (Fig. 5A and B), Q27/A70 was found to be more resistant to oxidation with respect to the K27/A70 variant. Conversely, if hydrogen peroxide was used as the oxidizing agent, the K27/A70 variant was found to be more resistant (Fig. 5C and D).

A molecular modeling study was carried out comparing the crystal structures of human CDA (1MQ0) and murine (2FR5) [33,34] in which the residue at position 27 is Q and K, respectively. This study suggested that the K27/A70 variant makes a strong ionic interaction with a glutamate residue located at position 24 (Figs. 7 and 8A), therefore it may be supposed that K27/A70 variant is more resistant to oxidizing agent H_2O_2 of Q27/A70, because of its greater structural rigidity due to an ionic interaction with the residue E24. This interaction may be lost if K27 is transformed into chloramines derivative, which, in contrast,

rejects electrostatically E24. To verify this hypothesis a CDA E24Q mutant was generated to evaluate the role of the interaction K27-E24 on enzyme functionality.

The supposed higher structural rigidity of the K27/A70 variant with respect to the Q27/A70 variant is also supported by the behavior of the mutant E24Q in presence of the oxidizing agents. When compared to the K27/A70 variant (Fig. 6), the E24Q mutant showed a larger sensitivity to hydrogen peroxide, which is consistent with the hypothesized loss of “protective” effect of the ionic interaction K27–E24, and a lower sensitivity to NaOCl, in line with the hypothesis that the chloramine derivative of K27 has a negative interaction with E24 (Fig. 8C).

The hypothesis of the increased structural rigidity of the K27/A70 variant, due to the ionic bond that K27 establishes with E24, is also supported by data from the van't Hoff plot, which indicates that a conformational change occurs at a temperature of about 35 °C that leads to a strong interaction with the substrate deoxycytidine. Enthalpically optimized binding affinities arise mostly from the formation of stereochemically specific hydrogen bonds, in addition to van der Waals interactions. Thus, selectivity is enhanced when hydrogen bond formation predominates [46].

Moreover, the loss of rigidity of the E24Q mutant is remarkably evident from the similarity of the behavior of this mutant with the Q27/A70 variant, shown by both the van't Hoff and Eyring plots (Figs. 3D and 4D). Notably, the E24Q mutant increased its activity above 50 °C and showed an optimal temperature around 65 °C. However, over this temperature the activity decreases substantially. The E24Q mutant CDA showed a low catalytic efficiency when compared to the functional variants K27/A70 and Q27/A70, which is most likely due to impaired substrate recognition, since K_m and K_i values, for substrates and inhibitors respectively, were shifted to higher values, whereas the V_{max} values were unaffected. In conclusion, this study supports the hypotheses that:

1. The K27/A70 variant may be characterized by more structural rigidity with respect to the Q27/A70, due to the ionic interaction that the lysine residue at position 27 establishes with a glutamate residue at position 24.
2. The Q27/A70 variant is a more efficient catalyst towards natural substrates and towards the antileukemic agent, cytarabine (Ara-C), indicating that this prodrug may be less effective on patients carrying the 79A>C SNP.
3. The CDA inhibitors 5-F-zebularine and tetrahydrouridine are more effective on the Q27/A70 variant, indicating that these inhibitors may be administered to the patient carrying the 79A>C SNP at lower doses.
4. The K27/T70 variant showed low catalytic efficiency toward all the analyzed substrates. This may indicate that patients carrying the 208G>A SNP have a better response with chemotherapeutic treatments based on nucleoside cytosine analogs. However it is necessary to take into account that the decreased deaminase activity may lead to an increased plasma level of these prodrugs, which may lead to severe drug toxicity [23].

Acknowledgments

The part of this work directed by Dr. Costanzi was initiated at the National Institute of Diabetes and Digestive and Kidney Diseases of the National Institutes of Health (SC and SV) and concluded at American University (SC and BW) and the University of Santiago de Compostela (SV). The authors acknowledge support by the Intramural Research of the National Institute of Diabetes and Digestive and Kidney Diseases of the National Institutes of Health (SC and SV), American University (SC and BW), and the Angeles Alvaríño program from Xunta de Galicia, Spain (SV).

Abbreviations

CDA	cytidine deaminase
SNP	Single Nucleotide Polymorphisms
CdR	2'-deoxycytidine
CR	cytidine
2'3'-CdR	2',3'-dideoxycytidine
Ara-C	1- β -D-arabino furanosylcytosine or cytarabine
Aza-CdR	5'-azadeoxycytidine
6-aza-CR	6-azacytidine
dFdC	2',2'-difluorodeoxycytidine or gemcitabine
fazarabine	1- β -D-arabinofuranosyl-5-azacytosine
THU	tetrahydrouridine
DTT	dithiothreitol dithiothreitol
IPTG	isopropyl-thio- β -D-galactopyranoside
EDTA	ethylenediaminetetraacetic acid

References

- Vincenzetti S, Quadri B, Mariani P, De Sanctis G, Cammertoni N, Polzonetti V, Pucciarelli S, Natalini P, Vita A. *Proteins*. 2008; 70:144–156. [PubMed: 17640070]
- Vincenzetti S, Carpi FM, Vita A. *Curr Top Pept Protein Res*. 2009; 10:1–22.
- Micozzi D, Pucciarelli S, Carpi FM, Costanzi S, De Sanctis G, Polzonetti V, Natalini P, Santarelli IF, Vita A, Vincenzetti S. *Int J Biol Macromol*. 2010; 47:471–482. [PubMed: 20637228]
- Laliberté J, Momparler RL. *Cancer Res*. 1994; 54:5401–5407. [PubMed: 7923172]
- Ho DH. *Cancer Res*. 1973; 33:2816–2820. [PubMed: 4518302]
- Kühn K, Bertling WM, Emmrich F. *Biochem Biophys Res Commun*. 1993; 190:1–7. [PubMed: 8422236]
- Mejer J, Mortensen BT. *Leuk Res*. 1988; 12:405–409. [PubMed: 3164086]
- Bøyum A, Løvhaug D, Seeberg E, Nordlie EM. *Exp Hematol*. 1994; 22:208–214. [PubMed: 7507861]
- Gran C, Bøyum A, Johansen RF, Løvhaug D, Seeberg E. *Blood*. 1998; 91:4127–4135. [PubMed: 9596658]
- Kassimos D, Kirwan JR, Kyle V, Hazleman B, Dieppe P. *Clin Exp Rheumatol*. 1995; 13:641–644. [PubMed: 8575145]
- Lavelle D, Vaitkus K, Ling Y, Ruiz MA, Mahfouz R, Ng KP, Negrotto S, Smith N, Terse P, Engelke KJ, Covey J, Chan KK, Desimone J, Sauntharajah Y. *Blood*. 2012; 119:1240–1247. [PubMed: 22160381]
- Teng YS, Anderson JE, Giblett ER. *Am J Hum Genet*. 1975; 27:492–497. [PubMed: 50738]
- Watanabe S, Uchida T. *Biochim Biophys Acta*. 1996; 1312:99–104. [PubMed: 8672545]
- Kirch HC, Schroder J, Hoppe H, Esche H, Seeber S, Schutte J. *Exp Hematol*. 1998; 26:21–425.
- Gilbert JA, Salavaggione OE, Ji Y, Pelleymounter LL, Eckloff BW, Wieben EB, Ames MM, Weinshilboum RM. *Clin Cancer Res*. 2006; 12:1794–1803. [PubMed: 16551864]
- Carpi FM, Vincenzetti S, Micozzi D, Vita A, Napolioni V. *Mol Biol Rep*. 2010; 37:3363–3368. [PubMed: 19941076]

17. Yue L, Saikawa Y, Ota K, Tanaka M, Nishimura R, Uehara T, Maeba H, Ito T, Sasaki T, Koizumi SA. Functional single-nucleotide polymorphism in the human cytidine deaminase gene contributing to ara-C sensitivity. *Pharmacogenetics*. 2003; 13:29–38. [PubMed: 12544510]
18. Xu J, Zhou Y, Zhang J, Chen Y, Zhuang R, Liu T, Cai W. *Clin Chim Acta*. 2012; 413:1284–1287. [PubMed: 22546611]
19. Vincenzetti S, Mariani PL, Cammertoni N, Polzonetti V, Natalini P, Quadrini B, Volpini R, Vita A. *Protein Eng Des Sel*. 2004; 17:871–877. [PubMed: 15713780]
20. Fukunaga AK, Marsh S, Murry DJ, Hurley TD, McLeod HL. *Pharmacogenom J*. 2004; 4:307–314.
21. Iyer SN, Tilak AV, Mukherjee MS, Singhal RS. *Biochem Genet*. 2012; 50:684–693. [PubMed: 22580794]
22. Fitzgerald SM, Goyal RK, Osborne WR, Roy JD, Wilson JW, Ferrell RE. *Hum Genet*. 2006; 119:276–283. [PubMed: 16446974]
23. Yonemori K, Ueno H, Okusaka T, Yamamoto N, Ikeda M, Saijo N, Yoshida T, Ishii H, Furuse J, Sugiyama E, Kim SR, Kikura-Hanajiri R, Hasegawa R, Saito Y, Ozawa S, Kaniwa N, Sawada J. *Clin Cancer Res*. 2005; 11:2620–2624. [PubMed: 15814642]
24. Sugiyama E, Kaniwa N, Kim SR, Hanajiri RK, Hasegawa R, Mackawa K, Saito Y, Ozawa S, Sawada J, Kamatani N, Furuse J, Ishii H, Yoshida T, Ueno H, Okusaka T, Saijo N. *J Clin Oncol*. 2007; 28:32–42. [PubMed: 17194903]
25. Ciccolini J, Dahan L, André N, Evrard A, Duluc M, Blesius A, Yang C, Giacometti S, Brunet C, Raynal C, Ortiz A, Frances N, Iliadis A, Duffaud F, Seitz JF, Mercier C. *J Clin Oncol*. 2010; 28:160–165. [PubMed: 19933910]
26. Ciccolini J, Mercier C, Dahan L, André N. *Nat Rev Clin Oncol*. 2011; 8:439–444. [PubMed: 21304503]
27. Wong A, Soo RA, Yong WP, Innocenti F. *Drug Rev*. 2009; 41:77–88.
28. Chabot GG, Bouchard J, Momparler RL. *Biochem Pharmacol*. 1983; 32:1327–1328. [PubMed: 6189497]
29. Momparler RL, Onetto-Pothier N, Momparler LF. *Leuk Res*. 1990; 14:755–760. [PubMed: 1700231]
30. Laliberté L, Marquez VE, Momparler RL. *Cancer Chemother Pharmacol*. 1992; 30:7–11. [PubMed: 1375134]
31. Eliopoulos N, Courmoyer D, Momparler RL. *Cancer Chemother Pharmacol*. 1998; 42:373–378. [PubMed: 9771951]
32. De Clerq E. *Curr Med Chem*. 2001; 8:1543–1572. [PubMed: 11562282]
33. Chung SJ, Fromme JC, Verdine GL. *J Med Chem*. 2005; 48:658–660. [PubMed: 15689149]
34. Teh H, Kimura M, Yamamoto M, Tanaka N, Yamaguchi I, Kumasaka T. *Biochemistry*. 2006; 45:7825–7833. [PubMed: 16784234]
35. Vincenzetti S, Cambi A, Neuhard J, Garattini E, Vita A. *Protein Exp Purif*. 1996; 8:247–253.
36. Bradford MM. *Anal Biochem*. 1976; 72:248–254. [PubMed: 942051]
37. Laemmli UK. *Nature*. 1970; 227:680–685. [PubMed: 5432063]
38. Kurella EG, Tyulina OV, Boldirev AA. *Cell Mol Neurobiol*. 1999; 19:133–140. [PubMed: 10079972]
39. Schrödinger Suite. Schrödinger, LLC; New York, NY, USA: 2012.
40. Baker JA, Wickremsinhe E, Li CH, Oluyedun OA, Dantzig AH, Hall SD, Qian YW, Ring BJ, Wrighton SA, Guo Y. *Drug Metab Dispos*. 2013; 41:541–545. [PubMed: 23230131]
41. Kreis W, Chan K, Budman DR, Schulman P, Allen S, Weiselberg L, Lichtman S, Henderson V, Freeman J, Deere M, Andreeff M, Vinciguerra V. *Cancer Res*. 1988; 48:1337–1342. [PubMed: 3342412]
42. Wang L, Tharp S, Selzer T, Benkovic SJ, Kohen A. *Biochemistry*. 2006; 45:1383–1392. [PubMed: 16445280]
43. Tanio M, Inoue S, Yokota K, Seki T, Tuzi S, Needleman R, Lanyi JK, Naito A, Saitô H. *Biophys J*. 1999; 77:431–442. [PubMed: 10388769]

44. Edwards SJ, Soudackov AV, Hammes-Schiffer S. *J Phys Chem B*. 2010; 114:6653–6660. [PubMed: 20423074]
45. Wong KF, Selzer T, Benkovic SJ, Hammes-Schiffer S. *Proc Natl Acad Sci USA*. 2005; 102:6807–6812. [PubMed: 15811945]
46. Freire E. *Drug Discov Today: Technol*. 2004; 1:259–295.

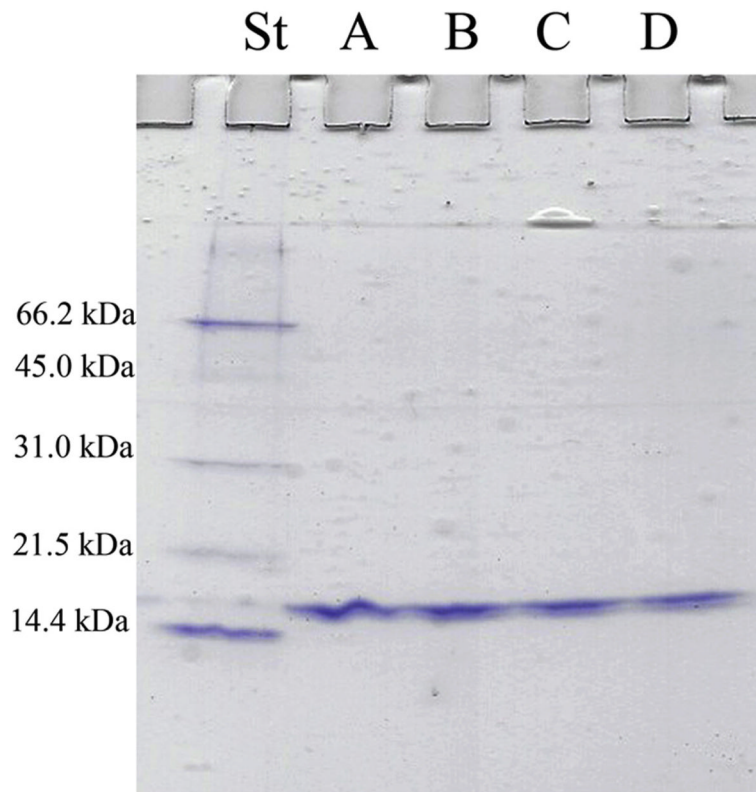


Fig. 1. 15% SDS-PAGE of purified CDA variants, and E24Q. (A) Q27/A70, (B) K27/A70, (C) K27/T70, (D) E24Q, st: Bio-Rad low molecular weight standard (97.4 kDa, phosphorylase b; 66.2 kDa, bovine serum albumin; 45.0 kDa, ovalbumin; 31.0 kDa, carbonic anhydrase; 21.5 kDa, soybean trypsin inhibitor; 14.4 kDa, lysozyme).

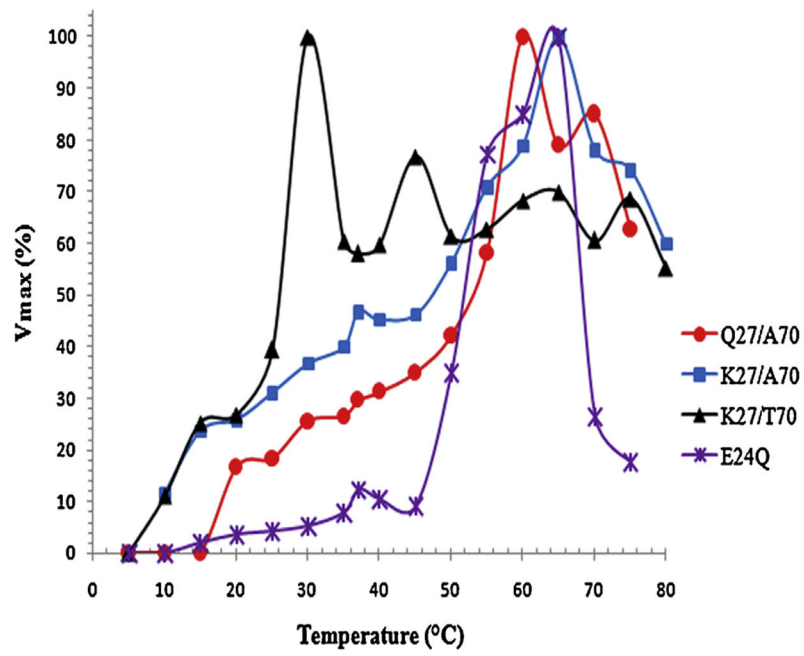


Fig. 2. Temperature effect on V_{\max} (%) of Q27/A70, K27/A70, K27/T70 functional variants and E24Q mutant enzyme.

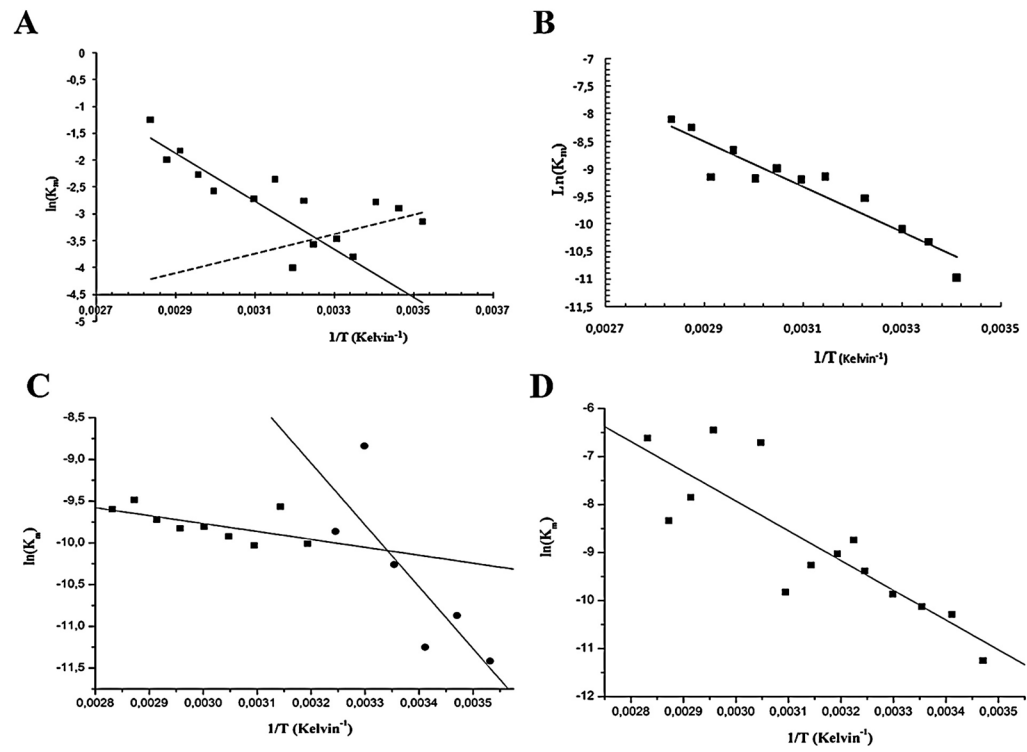


Fig. 3. Temperature effect on K_m (van't Hoff plots) of K27/A70 (A), Q27/A70 (B), K27/T70 (C) and E24Q (D).

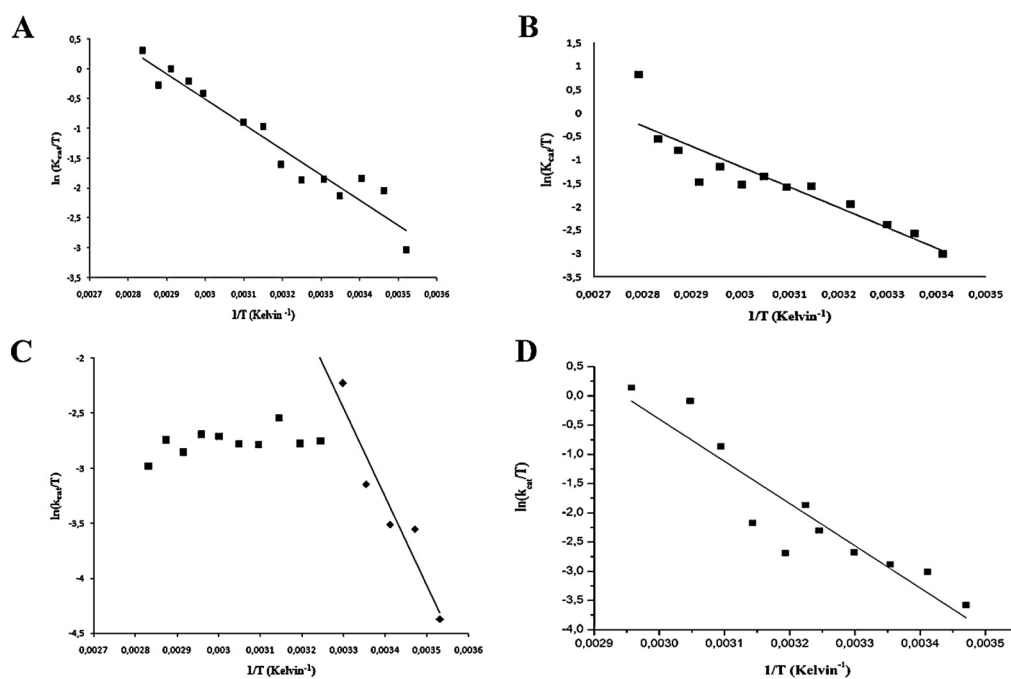


Fig. 4. Temperature effect on $\ln(k_{cat}/T)$ (Eyring plots) of K27/A70 (A), Q27/A70 (B), K27/T70 (C) and E24Q (D).

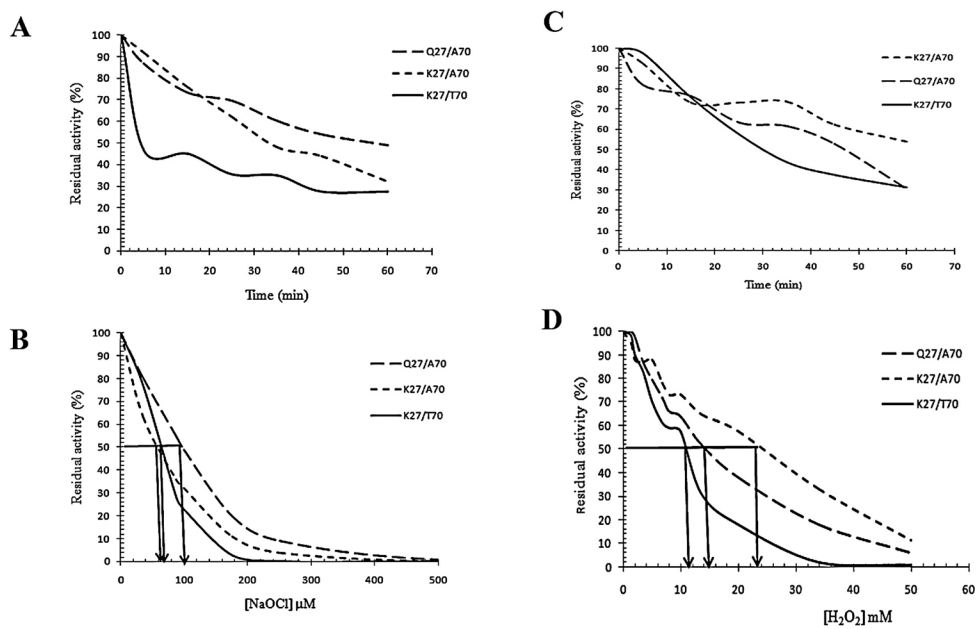


Fig. 5. Effect of sodium hypochlorite and hydrogen peroxide on Q27/A70, K27/A70, K27/T70: (A) time-dependent inhibition by a fixed NaOCl concentration (100 μM); (B) inhibiting effect of NaOCl; (C) time-dependent inhibition by a fixed H₂O₂ concentration (10 mM); (D) inhibiting effect of H₂O₂.

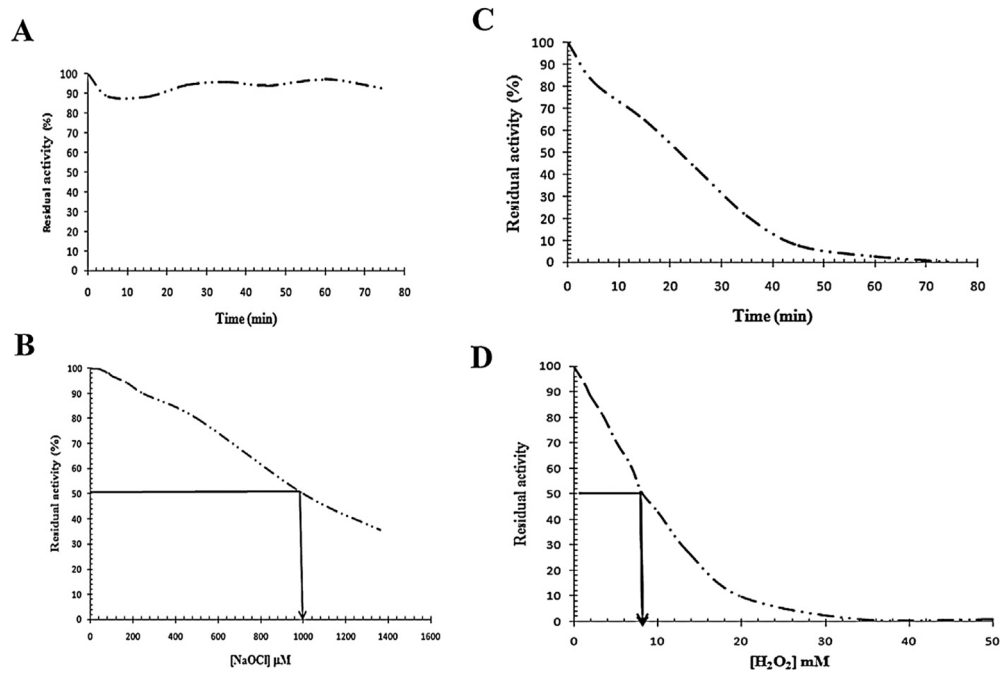


Fig. 6. Effect of sodium hypochlorite and hydrogen peroxide on E24Q: (A) time-dependent inhibition by a fixed NaOCl concentration (100 μM); (B) inhibiting effect of sodium hypochlorite; (C) time-dependent inhibition by a fixed H₂O₂ concentration (10 mM); (D) inhibiting effect of hydrogen peroxide.

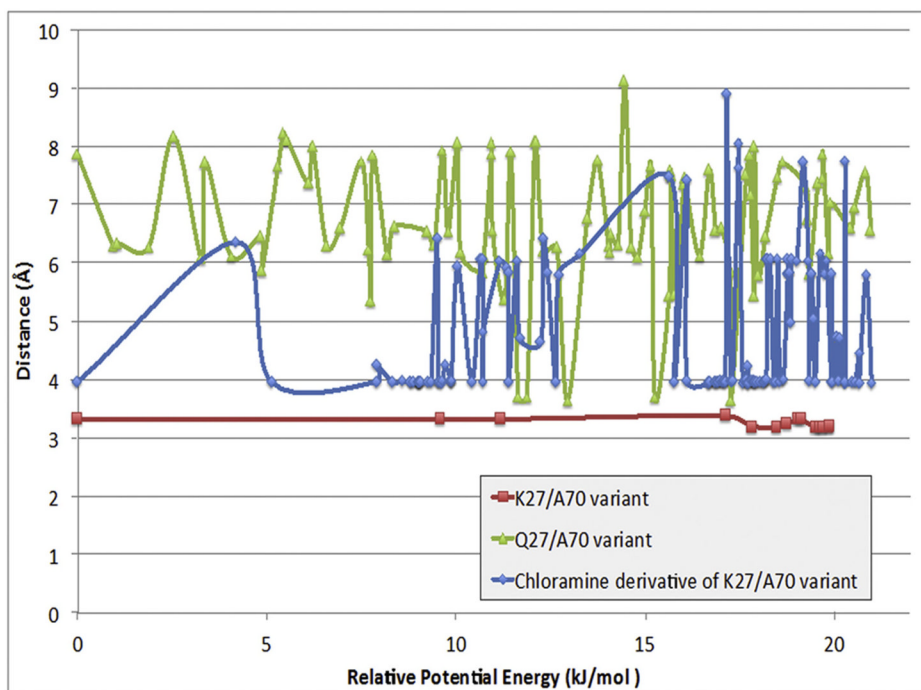


Fig. 7. Distances between the nitrogen atom of the side chain of Q27 or K27 and the carboxyl carbon atom of E24 for all the conformations generated through our Monte Carlo conformational searches.

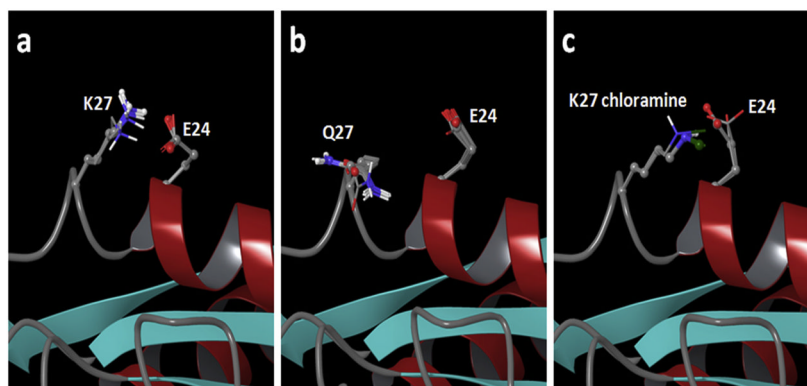


Fig. 8. Most energetically stable structures resulting three Monte Carlo conformational searches conducted to probe the local molecular interactions found in the K27/A70 and Q27/A70 variant. The figures shows the K27/A70 variant (Panel A) shows an ionic interaction between K27 and E24, which is absent in the Q27/A70 variant (Panel B) as well as the K27/A70 variant in which K27 is modified to its chloramine derivative (Panel C).

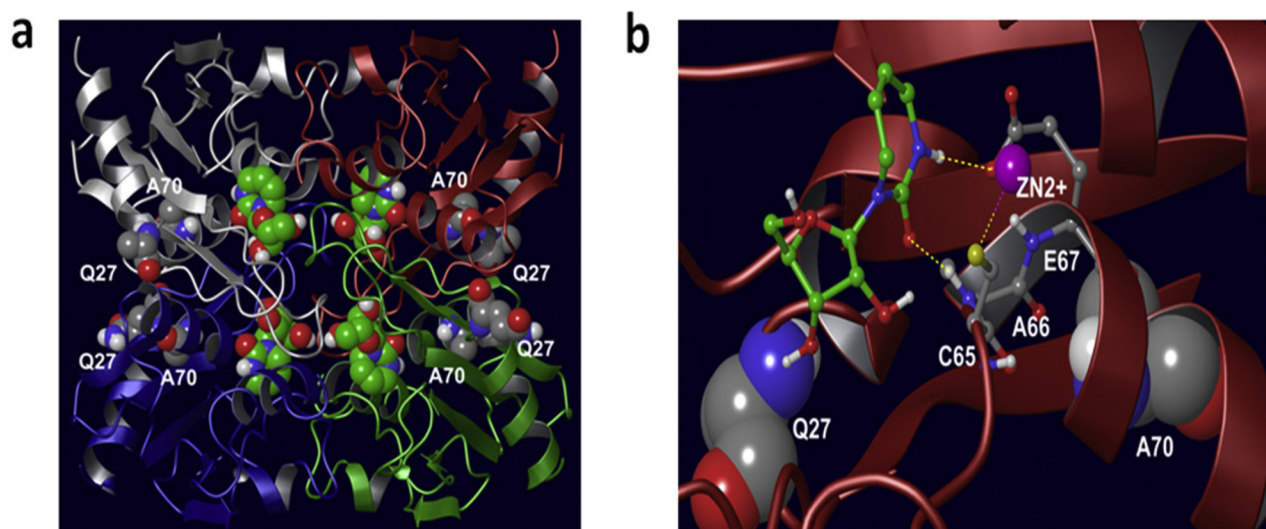


Fig. 9. Figure of the crystal structure of the Q27/A70 variant of the human CDA (2MQ0, 34) showing the location of Q27 and A70 with respect to the catalytic site. Panel A: view of the CDA tetramer. Panel B: close-up of the catalytic site.

Table 1

List of the primers used in site-directed mutagenesis experiments.

Mutation	Primer^a	Plasmid
A70T (K27/T70)	5'primer: 5'-GCTGAACGGACCA CT ATCCAGAAGGCCGTC-3' 3'primer: 5'-GACGGCCTTCTGGATA AGT GGTCCGTTTC-3'	pTrcHUMA70T
E24Q	5'primer: 5'-GCTCCAGCA AG GCCAAGAAGTCAGC-3' 3'primer: 5'-GCTGACTTCTTGGCCTGCTGGGAGC-3'	pTrcHUME24Q

^aMutated codons are indicated in bold.

Table 2

Residue presents (in bold) in each variant/mutant CDA.

Variant/mutant	Residue present
Q27/A70	E24, Q27 , A70
K27/A70	E24, K27 , A70
K27/T70	E24, K27, T70
E24Q	Q24 , K27, A70

Table 3

Kinetic parameters for substrates of CDA variants Q27/A70, K27/A70, K27/T70 and mutant E24Q.

Substrate ^a	K27/A70			Q27/A70			K27/T70			E24Q		
	K_m (μ M)	V_{max} (U/mg) ^b	V_{max}/K_m	K_m (μ M)	V_{max} (U/mg) ^b	V_{max}/K_m	K_m (μ M)	V_{max} (U/mg) ^b	V_{max}/K_m	K_m (μ M)	V_{max} (U/mg) ^b	V_{max}/K_m
CdR	40.0	45.5	1.14	37.4	55.0	1.47	60.0	2.82	4.70×10^{-2}	223	56.4	0.25
CR	42.0	53.0	1.26	17.6	73.5	4.18	90.0	5.19	5.76×10^{-2}	212	57.3	0.27
Ara-C	110	31.0	0.17	59.6	80.5	1.35	110	1.29	1.12×10^{-2}	347	31.5	0.091
2',3'-CdR	Not substrate	Not substrate	Not substrate	Not substrate	Not substrate	Not substrate	Not substrate	Not substrate	Not substrate	Not substrate	Not substrate	Not substrate
5-Aza-CdR	74.0	31.0	0.40	210	21.5	0.10	330	1.38	4.20×10^{-3}	224	7.72	0.034
6-aza-CR	1014	43.8	0.043	29,850	620	0.020	328	0.32	9.70×10^{-4}	n.d.	n.d.	n.d.
Fazarabine	2300	148	0.064	4270	89.0	0.021	670	1.10	1.60×10^{-3}	n.d.	n.d.	n.d.

^aCdR: 2'-deoxycytidine; CR: cytidine; Ara-C: cytosine arabinoside; 5-Aza-CdR: 5-aza deoxycytidine; 6-aza-CR: 6-azacytidine; fazarabine: 1- β -D-arabinofuranosyl-5-azacytosine; n.d.: not determined.

^bUnits are defined as micromoles of substrate deaminated per minute at 37 °C.

Table 4

Inhibition constants of Q27/A70, K27/A70, K27/T70 and E24Q.

Inhibitors	K27/A70 $K_i (\times 10^{-5} \text{ M})^a$	Q27/A70 $K_i (\times 10^{-5} \text{ M})^a$	K27/T70 $K_i (\times 10^{-5} \text{ M})^a$	E24Q $K_i (\times 10^{-5} \text{ M})^a$
Zebularine	0.10	0.25	0.36	0.50
5-F-zebularine	0.03	0.005	0.027	0.029
Tetrahydrouridine	0.015	0.004	0.034	0.079
Tetrahydro-2'-deoxyuridine	0.004	0.026	0.026	n.d.
3-Deaza-cytidine	0.05	0.18	0.24	0.29
Pseudoisocytidine-HCl	2.80	4.60	6.00	n.d.

^aInhibition constants were obtained from the double-reciprocal plots of the deamination of deoxycytidine in the presence and absence of the inhibitors. All the inhibitors were competitive.